J. Appl. Cryst. (1997). **30**, 1140–1147

SANS at Pulsed Neutron Sources: Present and Future Prospects†

R. K. HEENAN,* J. PENFOLD AND S. M. KING

ISIS Facility, Rutherford Appleton Laboratory, Chilton, Didcot, Oxon, England. E-mail: rkh@isise.rl.ac.uk

(Received 23 July 1996; accepted 3 February 1997)

Abstract

Small-angle diffraction with a pulsed neutron source, using time-of-flight analysis to separate neutrons of different wavelengths, offers a very wide simultaneous Q range coupled to good Q resolution. Data reduction to allow for wavelength-dependent effects may be achieved as a matter of routine. The cold neutron flux available from accelerator-based neutron sources does not yet fully match that of the most intense reactor sources. Simulations show that the performance of proposed future instrumentation would be largely complementary to that of the best fixed-wavelength instruments.

1. Introduction

Application of the SANS technique to a wide range of scientific disciplines has been reviewed by many authors (for example Windsor, 1988; Teixeira, 1992). Though there are many reactor neutron sources which have small-angle instruments, only five laboratories operate time-of-flight diffractometers with pulsed neutron sources. Four accelerator-based instruments, LQD at LANSCE, Los Alamos, SAD (and more recently SAND) at IPNS, Chicago, SAN at KEK, Japan (Ishikawa *et al.*, 1986), and LOQ at ISIS, England, have been reviewed by Seeger (1995). The pulsed nuclear reactor source IBR-2, at JINR, Dubna, Russia, has a SANS beamline with an extremely high incident flux (Ostanevich, 1988), though it suffers from a high background between pulses. Conventional reactor source instruments have also been run in time-of-flight mode with a broad wavelength band-chopped beam, for example at CEN, Saclay (Cotton & Teixeira, 1986). The growing interest in pulsed-source SANS instrumentation is due to the advantages of a wide range of scattering vectors, and hence sizes of scattering object, that can be accessed in a single measurement, compared with using a fixed incident wavelength in a conventional system. This is of particular importance in the study of dynamic systems, colloids and oriented samples.

A comparison of the relative merits of fixed-wavelength and pulsed-source SANS instruments that exist today, or that might exist in the future, requires careful consideration of the scientific goals of an experiment in terms of the Q range and Q resolution that are required. In order to make such a comparison, it is necessary to understand something of the characteristics of a pulsed source, the data-reduction process and the nature of the Q-space resolution function. These are considered in turn below, with some typical data from LOQ at ISIS, which may be considered as representative of other pulsed-source SANS instruments.

2. Characteristics of pulsed neutron sources

Accelerator-based pulsed neutron sources use spallation of nuclei in a high atomic number target as an energy efficient means to produce neutrons. At ISIS, an 800 MeV, 200 μA proton beam is delivered in 50 Hz pulses to a tantalum target cooled by heavy water. Both reactor and pulsed-source neutron sources use cryogenic moderators to slow their neutrons to more useful energies. The pulsed-source moderator emits pulses of a broad band of neutron wavelengths λ (Å), which then disperse in time T (ms) along flight path L (m) such that:

$$T = (m/h)L\lambda = L\lambda/0.2528 \quad \text{or} \quad \lambda \simeq 4T/L. \qquad (1)$$

The maximum range of wavelengths that may be used before 'frame overlap' occurs, when the fast neutrons from one pulse overtake the slow neutrons of the preceding pulse, is $\lambda_{max} - \lambda_{min} \simeq 4T_p/L_D$, where T_P is the time between pulses and L_D is the distance from the moderator to the final SANS detector.

The 50 Hz repetition rate of ISIS is higher than that of other pulsed accelerator-based neutron sources. A mechanical disc chopper, with a variable opening angle, is used to define the wavelengths used and, in normal operation, to remove alternate pulses. This doubles T_P from 20 to 40 ms, to allow λ_{max} = 10 Å at L = 15 m, but means that LOQ's detectors must count through a 'prompt' background spike of fast neutrons associated with the removed pulse, which comes more or less directly from the neutron producing target. In general, when choosing λ_{min} and λ_{max} for particular detector distances, the possibility of frame overlap and the arrival times of prompt background spikes must be considered.

The LOQ beamline is shown to scale in Fig. 1, where substantial radiation shielding out to a distance of 6 m from the moderator may be noted, within which it is

† This paper was presented at the Tenth International Conference on Small-Angle Scattering, Campinas, Brazil, 21–26 July, 1996.

difficult to place beamline components. The sample position is at around 11.1 m, followed by a space for a new 'high-angle' detector and a 4 m evacuated flight path to a 64 cm square two-dimensional ^{3}He gas detector.

In practical terms, the minimum wavelength, λ_{min}, used is around 1 Å, as a result of detector efficiencies and background suppressing filters. On LOQ, however, a super-mirror Soller bender is used to deflect the neutron beam through 24 mrad in order to reduce the fast-neutron background at the main detector. The critical angle of this device, together with a strong aluminium Bragg edge, give a useful λ_{min} of 2.2 Å. A monitor spectrum recorded with a low-efficiency scintillator detector on LOQ is shown in Fig. 2, which displays several dips, caused by Bragg scattering by aluminium vacuum windows, and a prompt spike at 20 ms, which in this monitor spectrum requires interpolation.

3. Pulsed-source SANS data reduction

The data-reduction process requires the combination of neutron scattering cross sections obtained at different wavelengths. Wavelength-dependent corrections are required for the incident spectrum shape, detector efficiency and sample transmission. The process has been described in some detail by Seeger & Hjelm (1991), so will only be outlined here, in a form slightly modified to suit LOQ at ISIS.

The number of neutrons of wavelength λ arriving per unit time at a detector element of area A, at a sample–detector distance L and radius R from the diffractometer axis, when the sample has a coherent SANS cross section $\partial\Sigma(Q)/\partial\Omega$ (in cm^{-1}), is given by:

$$I(R, \lambda) = I_0(\lambda)[\partial\Sigma(Q)/\partial\Omega]\Delta\Omega(R)tT(\lambda)\eta(\lambda) \quad (2)$$

where $I_0(\lambda)$ is the incident beam current in neutrons s^{-1}, t is the sample thickness in cm, $\Delta\Omega(R) = A/L^2$ is the solid angle of the detector element, $T(\lambda)$ is the transmission of the sample and $\eta(\lambda)$ is the efficiency of the detector. In a conventional fixed-wavelength SANS experiment, the cross section $\partial\Sigma(Q)/\partial\Omega$ is determined by using a 'flat scatterer' of 'known' cross section, often vanadium or water, as a measure of the term $\Delta\Omega(R)\eta(\lambda)$. The scattering vector Q is, as usual, $4\pi\sin(\theta/2)/\lambda$, where $\theta \simeq R/L$ is the scattering angle.

For a pulsed source it is difficult to find a calibration material that scatters strongly enough to give good counting statistics over the whole detector at every wavelength and for which the cross section is known. Instead, we use (2) directly by first determining the detector efficiency $\eta(\lambda)$ for the area detector, or rather its ratio to that for the incident beam monitor, $\eta_m(\lambda)$, which is all that is, in fact, required.

The ratio may be measured at the centre of the detector, by a sum $I_H(\lambda)$ over the incident-beam profile with the beam stop removed, with corresponding monitor counts $M_H(\lambda)$. To avoid saturating the detector, a mask, of area A_H, is placed on the beam axis between the monitor, of area A_m, and the main detector. We then have a 'direct-beam' function:

$$D(\lambda) = I_H(\lambda)/M_H(\lambda) = [\eta(\lambda)/\eta_m(\lambda)](A_H/A_m). \quad (3)$$

Substituting in (2) gives, for monitor counts $M(\lambda)$:

$$\partial\Sigma(Q)/\partial\Omega = [I(R, \lambda)/M(\lambda)][1/T(\lambda)][A_H/D(\lambda)] \times [1/A_S t\Delta\Omega(R)]. \quad (4)$$

The direct-beam function $D(\lambda)$, shown in Fig. 3, also accounts for the adsorption by any windows in the beamline between the monitor and area detectors, such as the Bragg dips at short wavelengths caused by the vacuum window in front of the detector.

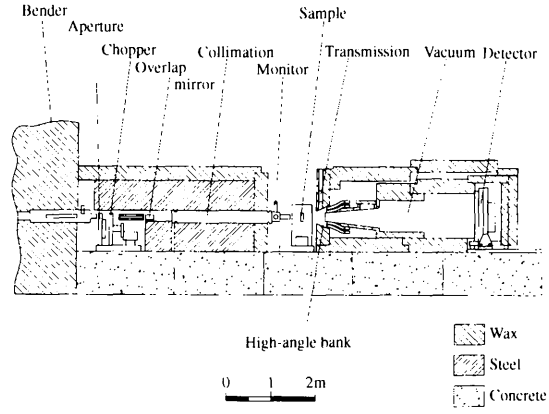

Fig. 1. Cross section of the LOQ SANS beamline at ISIS, including the substantial shielding around the neutron-producing target and moderators. The sample position is at 11.1 m from the moderator, a high-angle detector is at 11.6 m and the main detector is at 15.2 m. Two variable apertures define pinhole collimation. A super-mirror bender, a disc chopper and a nickel-coated silicon-wafer frame overlap mirror system define the wavelengths used.

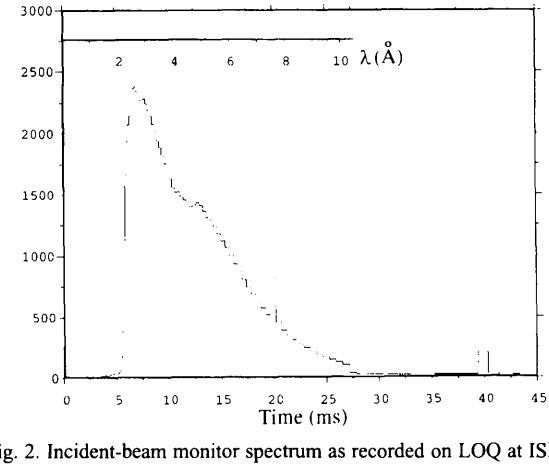

Fig. 2. Incident-beam monitor spectrum as recorded on LOQ at ISIS in time of flight, with corresponding wavelengths, selected by a 25 Hz rotating disc chopper. The spikes at 20 and 40 ms are 'prompt' fast-neutron background.

In accumulating the counts from the different radii and wavelengths which contibute to a given Q bin, the counts are weighted by the incident beam as it would be seen at the main detector, so that:

$$\partial\Sigma(Q)/\partial\Omega = (A_H/A_S t) \sum_{(R,\lambda\subset Q)} I(R,\lambda) \Big/ \sum_{(R,\lambda\subset Q)} [M(\lambda) \times T(\lambda)D(\lambda)\Delta\Omega(R)]. \quad (5)$$

The numerator is simply the number of neutrons appearing in a particular Q bin; therefore, it has an obvious statistical error.

The method of determining the $D(\lambda)$ and $\Delta\Omega(R)$ terms depends in detail on the type of detector in use. We assume that for the two-dimensional ORDELA ^{3}He gas detector on LOQ, at 4 m from the sample, the wavelength dependence of efficiency does not vary with position. The detector solid-angle term $\Delta\Omega(R)$ for each pixel is assumed to be independent of wavelength, and is measured experimentally with a neutron/gamma source placed at the sample position. A further measurement, using neutrons scattered from a sample through a mask of holes placed immediately in front of the detector, enables correction for detector edge effects in the time interval coded detector.

It should be noted that, except at the extreme limits of the Q range, the data included in a particular Q bin are obtained from an average of different wavelengths over a large area of the detector, so that local variations in detector efficiency tend to be averaged out.

The effective scaling constant A_H in (5) is routinely checked by fits to data from partially deuterated solid polystyrene samples of known cross section (Wignall & Bates, 1987).

The overlap of the cross section obtained from different wavelength bands is a sensitive check of the normalization and transmission corrections. A typical overlap plot is shown in Fig. 4 for a standard deuterated polystyrene sample in order to indicate the degree of reproducibility between cross sections at different wavelengths.

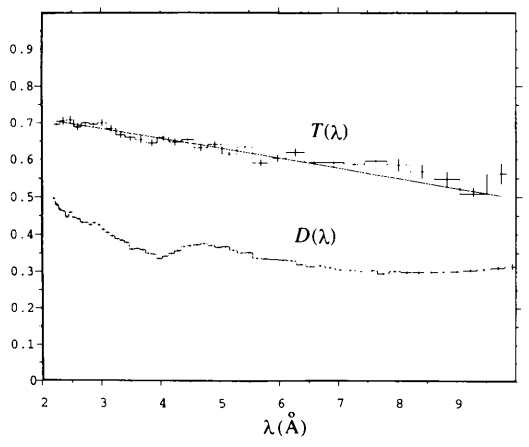

Fig. 3. A typical transmission measurement, $T(\lambda)$, from LOQ for the polymer data in Fig. 4. Direct-beam function, $D(\lambda)$, is used to correct for the wavelength dependence of detector efficiencies (see text).

Transmissions $T(\lambda)$ are recorded (in a few minutes on LOQ) by inserting a separate scintillator slab detector immediately after the sample while reducing the incident-beam diameter between the monitor and sample to 1 mm to reduce the count rate. An example is shown in Fig. 3.

Caution must be exercised when considering the 'incoherent' scattering from hydrogenous samples or when attempting to devise a suitable 'background sample' to subtract. A significant fraction of the 'incoherent' scattering from an hydrogenous sample is, in fact, multiple inelastic scattering, which on a time-of-flight instrument may arrive in a different time channel to its notional wavelength. The scattering observed after data reduction depends upon the sample, the relative detector efficiency at short wavelengths and the instrument configuration, and it is not necessarily flat in Q space (Ghosh & Rennie, 1990; Rennie & Heenan, 1992; Heenan & Rennie, 1994; Teixeira, 1992). The cold neutron beam is actually partially thermalized by hydrogen atoms in the sample; therefore, it is largely up-scattered to shorter wavelengths, as illustrated in Fig. 5, and hence tends to appear at higher Q. Closing the chopper disc opening on LOQ allows the instrument to be used as an inelastic spectrometer, with rather limited energy resolution and count rate.

4. Pulsed-source Q SANS resolution

With the exception of the SAD instrument at IPNS, which uses converging Soller collimation, pulsed-source SANS instruments have, to date, used simple 'pinhole' collimation similar to reactor-based instruments. The Q-space resolution has been discussed by a number of authors, including Mildner & Carpenter (1984), Pedersen *et al.* (1990), and Barker & Pedersen (1995), and has been applied to time-of-flight measurements by Mildner, Carpenter & Worcester (1986). The full width at half-maximum (FWHM) of the resolution function at small Q is given approximately by

$$\delta Q_{\rm FWHM} \simeq (2.35\pi/\lambda)\{R_1^2[(l+L_2)/L_1L_2]^2 + R_2^2[(L_1+l+L_2)/L_1L_2]^2 + (1/3)(\Delta R/L_2)^2 + (1/3)(R/L_2)^2(\Delta\lambda/\lambda)^2\}^{1/2} \quad (6)$$

where L_1 is the distance between the two beam-defining apertures, l is the distance from the second aperture to the sample, L_2 is the sample–detector distance and ΔR is the width of an annular ring at radius R on the detector. [A component perpendicular to Q is neglected here; see Pedersen *et al.* (1990).]

Except at the extremes of Q, scattering cross sections on a pulsed source are combinations of data from a range of wavelengths, each with a different resolution width. Numerical simulations show that the overall, appropriately averaged, resolution function is described well by a Gaussian with a broadened tail (Heenan, 1996). The broadening of the tail is attributed to the shorter wavelengths contributing to each Q. As may be seen in Fig. 6, the peak from the combined data is still relatively sharp, while its tail is broad. Where the best possible resolution is required, the summations in (5) may, post-experiment, reject channels that contribute adversely, notably the shorter wavelengths close to the beam stop, but at the expense of worse counting statistics.

The geometrical terms in (6) are the same for both fixed-wavelength and pulsed-source SANS and tend to dominate at small radius R. The wavelength uncertainty $\Delta\lambda$ in (6) for the two instrument types needs to be defined carefully. Throughout this work, δ refers to a FWHM, while Δ is the full width of a rectangular distribution and σ is a standard deviation. For a Gaussian distribution, such as from a velocity selector, $\sigma = \delta/[8\ln(2)]^{1/2} \simeq \delta/2.35$, and for a rectangular distribution, such as a time channel width, $\sigma = \Delta/12^{1/2} \simeq \Delta/3.46$.

On a pulsed source, there are contributions to $\Delta\lambda$ from the time channel width used in data acquisition and the spread of neutron wavelengths actually arriving at a given time due to the moderation process. For the 'decoupled' type of hydrogen moderator, used at ISIS or LANSCE, neutrons of a given wavelength have an asymmetric distribution with a relatively sharp leading edge followed by an exponentially decaying tail with time constant τ. If one assumes the leading edge to be vertical, then the mean and standard deviation of the distribution are both simply τ. The decay time τ increases from around 40 μs at 2 Å to saturate at around 100 μs at around 5.5 Å (Kiyanagi, Watanabe, Furusaka, Iwasa & Fujikawa, 1990; Kiyanagi, Watanabe & Iwasa, 1992). (The actual lengths of the proton pulses reaching the ISIS target are, for comparison, less than 1 μs.) The contribution of τ to $\delta\lambda$ actually decreases with increasing length of beamline according to (1).

Following this through for the detector distances on LOQ and convoluting with a generous time channel width of $\Delta t/t = 2.5\%$, gives, for example, on LOQ an effective $\delta\lambda/\lambda$ of approximately 2.6% FWHM at 2 Å and 2.0% FWHM at 10 Å. Some of the gain compared to a reactor instrument, of typically $\delta\lambda/\lambda = 10\%$ FWHM, is lost, however, since the resolution function (6) varies inversely with wavelength and the pulsed source tends to use shorter incident wavelengths. Thus the resolution $\delta Q/Q$ in the upper part of the Q range on LOQ is still around 7% FWHM, which is better than on most conventional instruments. Since it is well known that, at least for the geometric terms in (6), count rate varies inversely with the fourth power of Q space resolution (Mildner & Carpenter, 1984), the difference in resolution functions makes direct comparisons of performance difficult. This is further addressed below.

5. Development of pulsed-source flux

The liquid-hydrogen moderators used at ISIS and LANSCE for SANS experiments are both 'decoupled' from their respective surrounding neutron reflector. A slow-neutron adsorbing material surrounds much of the moderator, so that neutrons multiply scattered between the moderator and a surrounding Be or heavy-water 'reflector' are curtailed at low energy. A 'coupled' moderator has no slow-neutron adsorber, so the neutrons are able to almost completely thermalize to the temperature of the H atoms in the moderator. Together with a 'pre-moderator', a coupled moderator on existing facilities would have a cold neutron flux of around six times that of a decoupled moderator, but with increased

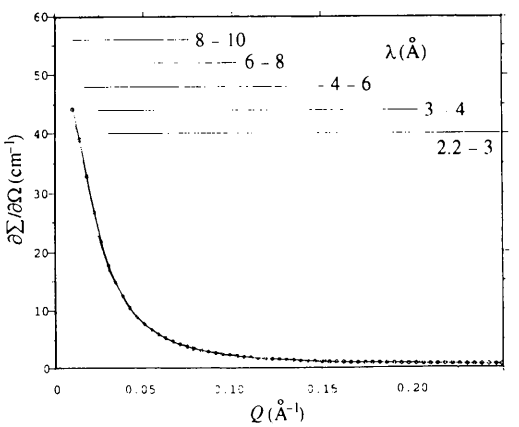

Fig. 4. Q ranges on the present LOQ main detector for different bands of neutron wavelength. The data below has lines for a 20% deuterated polystyrene sample reduced separately for each band, and for the full λ = 2.2–10 Å (circles).

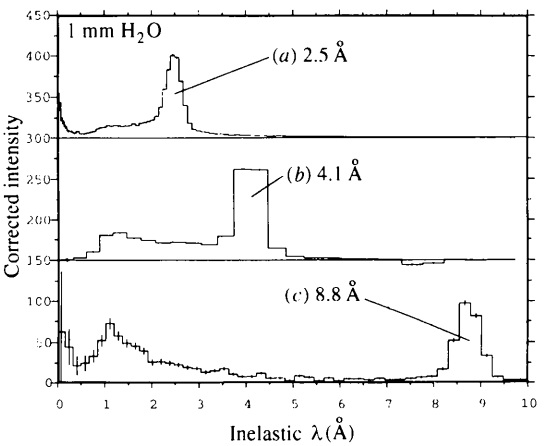

Fig. 5. Inelastic scattering spectra for 1 mm H_2O recorded on LOQ at different incident wavelengths, after correcting for backgrounds and approximately for detector efficiency (which is uncertain at very short wavelengths).

decay times τ (Kiyanagi *et al.*, 1990, 1992). The present moderators are a compromise to suit certain inelastic scattering spectrometers which must share their use. The pulse repetition frequency of existing sources, for example the 50 Hz of ISIS, further compromises the use of a broad band of cold-neutron wavelengths because of frame overlap considerations [(1)] to suit the use of higher energy neutrons. Despite these compromises, cold-neutron experiments on pulsed sources are, in general, already very competitive, as discussed by Carlile & Penfold (1995).

Fits of the data from an experimental simulation of a coupled hydrogen moderator (Kiyanagi *et al.*, 1990, 1992) suggest that decay times τ would be of the order of 100 μs at λ = 1 Å, increasing to saturate at around 300 μs above 3 Å. This would still provide an extremely well defined $\delta\lambda/\lambda$ of, for example at L = 10 m, 2.35% FWHM below 3 Å falling to 0.7% at 10 Å, or half these amounts at L = 20 m. More detailed calculations show that for SANS at short wavelengths and higher Q values, the tails of the Q space resolution function start to broaden asymmetrically to higher Q. This is due to the exponential tails of the moderator time distributions of shorter wavelengths which are still arriving at the detector. In most circumstances, however, this would not noticeably worsen the performance of a SANS instrument.

Predicted spectrum shapes for coupled and decoupled hydrogen moderators are shown in Fig. 7 [using data reported by Taylor (1992) and Perring *et al.* (1985)].

The present ISIS target dissipates some 160 kW of heat from an 800 MeV, 200 μA, proton beam, at 50 Hz. Design studies suggest that a target for a dedicated 10 Hz cold-neutron source could operate at 1 MW (Taylor, 1992), in order to gain a further factor of six in flux. With such an accelerator, the time-averaged flux of a coupled hydrogen moderator would be about one quarter that of the Institut Laue–Langevin (ILL), Grenoble, second cold source, used by D22. The implications of this for SANS are discussed in §6. At 10 Hz, frame overlap is not a significant problem as it only occurs for a 10 Å wavelength band at L = 40 m, or for a 20 Å band at L = 20 m; thus, the majority of the incident spectrum would always be available to the instrument.

If one compares the present LOQ instrument at ISIS, then a further improvement factor of about ten must be included. This includes a factor of two since the ISIS hydrogen moderator is located to the rear of the neutron target, not at the prime front position, and a factor of two for operation at 25 Hz, half the source frequency, as well as losses due to the super-mirror bender and frame overlap mirrors. This concurs with practical observations on similar samples that in the mid Q range, SANS on D11 at ILL has, at present, a gain in flux of typically some 25 over that of LOQ.

Further increases in flux of the order of two at a pulsed source might be possible by use of 'slab' geometry for the moderator rather than the present 'wing' arrangement. In the slab case, the moderator is directly in front of the neutron target, so a beamline receives a far greater fast-neutron background compared to that for 'wing' geometry, where the moderator is above or below the target. This might not be so severe a problem if a curved Soller bender or guide were to be used to remove SANS instruments from the direct line of sight of the moderator.

A solid methane rather than a hydrogen moderator could potentially increase flux by a further factor of four, due to a higher density of hydrogen atoms. To date, however, the use of methane cryogenic moderators has posed many difficulties due to radiation-induced chemistry (Broome, Hogston, Holding & Howells, 1994).

There has been much recent discussion of the merits of a 'long-pulse' type of spallation neutron source, in which the proton pulses are stretched from a few μs to 1 or 2 ms

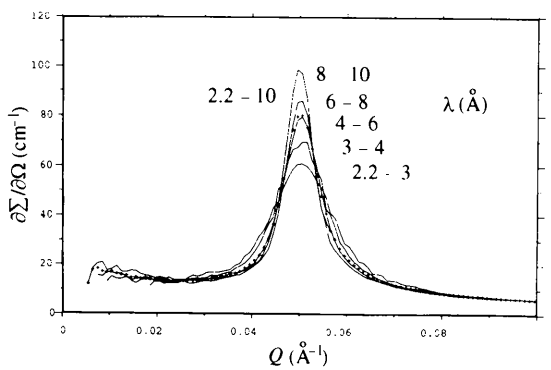

Fig. 6. Experimental data from LOQ, reduced in the wavelength bands as shown, for a lamellar system which happened to scatter at a Q value accessible to all the wavelengths used. Note that the composite data set (+++) remains sharp in the peak, but broadens in the tail due to inclusion of short wavelengths.

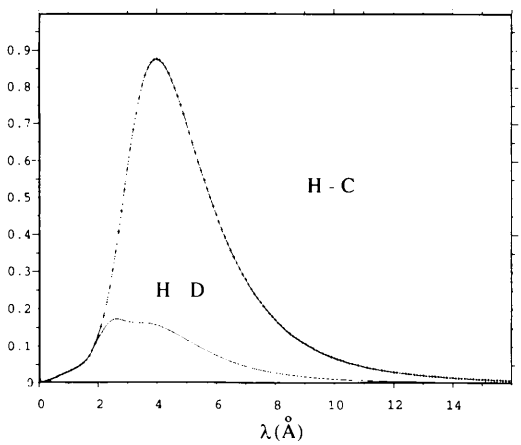

Fig. 7. Illustration of the increase in long-wavelength neutron flux expected on going from a 'decoupled' (H-D) to a coupled (H-C) liquid-hydrogen moderator. The spectra are reduced at short wavelength by assuming a neutron guide or bender of characteristic wavelength λ^* = 2 Å and the efficiency of a 1 mm thick scintillator detector.

(Mezei, 1994*a*,*b*; Pynn, 1995). Such long pulses would adversely affect the $\delta\lambda$ wavelength resolution, particulary at short wavelengths and/or flight paths, and would also produce very long 'prompt' background spikes. A long-pulse cold source, particularly at a high repetition rate which reduces the band width of neutrons used, would, for SANS, emulate what is already available at the best reactors but without the option for much improvement of $\delta\lambda$ resolution (Seeger, 1995). Given the 100–300 μs decay time of a coupled moderator, a more modest lengthening of the proton pulse could be tolerated by SANS instruments if this were to be accompanied by an increase in the power of the target.

6. Comparison of state of the art pulsed-source and fixed-wavelength SANS

As outlined above, a realistic estimate of cold-neutron production at a hypothetical 1 MW, 10 Hz, target would conservatively be around one quarter the time-averaged flux of the second cold source at ILL, which is presently the best available. A pulsed source is able, however, to use all of this flux simultaneously, whereas the reactor source must select only part of it. The relative merits of a SANS experiment on the two types of source depend, for count rate, on how much of the spectrum is used to acheive a particular scientific goal. The importance that should be ascribed to differences in Q range and Q resolution is even more difficult to quantify.

By way of illustration, Figs. 8–10 demonstrate the Q range, counts per Q bin and Q resolution of a hypothetical pulsed-source instrument '10/5/5' using the coupled hydrogen moderator spectrum of Fig. 7. This has a neutron guide within an expected 10 m of bulk shield for a 1 MW target (*cf.* 6 m in Fig. 1), followed by 5 m of collimation, a sample and a 5 m flight path to a detector of 1 m diameter (notionally a zinc sulfide scintillator array with 5 mm resolution). Fixed-wavelength instruments at λ = 4.5 and 9 Å are compared, for the *same* number of detected neutrons, and assuming in the resolution calculation a 10% FWHM velocity selector. The resolution, calculated using (6) and (5), is only approximate, but the differences between the types of source should be representative of a real situation.

First note that the distribution of counts across the Q space for a flat scatterer is rather different for the two types of source (Fig. 8). The same type of plot is, of course, produced for longer flight paths and lower Q's. The count rate of the pulsed-source SANS always falls off at the extremes of Q, simply because, as seen in Fig.

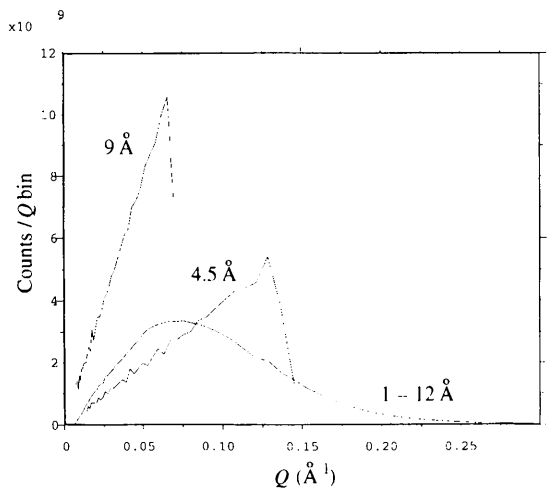

Fig. 8. Counts *versus* Q for a flat scatterer on a hypothetical SANS instrument, '10/5/5', with a 1 m diameter detector at 5 m from the sample. The line λ = 1–12 Å is for a 10 Hz pulsed source, with the H-C spectrum of Fig. 7, while the lines λ = 4.5 and 9 Å are for a fixed-wavelength instrument recording the same number of neutrons.

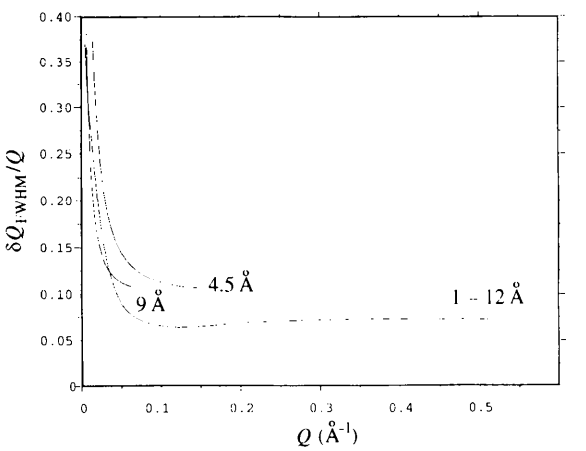

Fig. 9. Numerically computed mean Q resolution for the 10/5/5 hypothetical instrument of Fig. 8. The 4.5 and 9 Å fixed-wavelength versions assume a velocity selector of 10% FWHM, while the 1–12 Å pulsed instrument uses the H-C spectrum of Fig. 7 with a maximum 300 μs time constant for the tails of the moderator time distribution (see text for details).

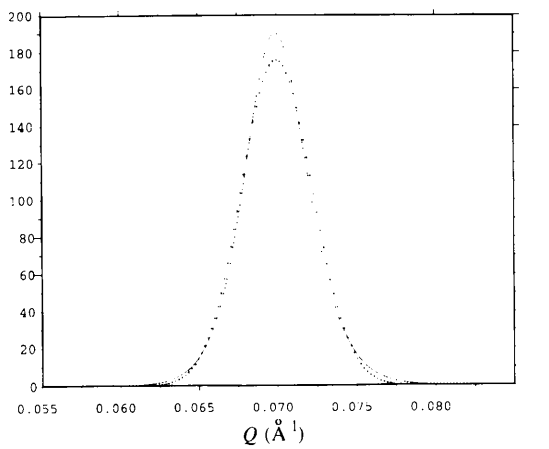

Fig. 10. A numerically computed resolution curve (line) for the 10/5/5 H-C pulsed instrument of Figs. 8 and 9, to illustrate the distortion of the curve away from a Gaussian when a broad range of wavelengths, 1–12 Å, is included (+++ is least-squares Gaussian fit). The H-D moderator gives very similar results at this Q. (*cf.* Fig. 6.)

4, only a small fraction of the available spectrum reaches these points. Thus, in general, pulsed-source SANS is often better suited to model fitting a wide Q range, rather than focussing on the extremes of Q for say 'Guinier' or 'Porod' type analyses. This also demonstrates that even a pulsed-source SANS instrument benefits from a moveable detector in order to optimize peak count rate to a region of interest.

The intrinsically good wavelength resolution of the pulsed source leads to the possibility of relatively good Q resolution over most of the Q range, which can only be matched on a reactor source by significantly reducing intensity.

If only a small Q measurement is required, from the longest wavelengths available, with not particularly good Q resolution, which in any case is dominated by geometrical terms at very small Q, then the reactor and pulsed sources would both be using roughly the same proportion of their spectrum and the reactor would have the higher count rate by a factor of four margin.

At higher Q values accessible by either most of the flux of the pulsed source or, say, by $\lambda = 4.5$ Å, around the peak of the moderator spectrum, a numerical integration of the H-C spectrum in Fig. 7 suggests that a reactor might use, say, 28% of its flux for $\delta\lambda/\lambda = 10\%$ FWHM. In this case, the count rates of the two instruments would be roughly equal. However, this should be regarded as an unfair comparison since the pulsed-source resolution is much better. Selecting instead a 2% FWHM for the reactor, the pulsed source would be better by a factor of at least four in count rate. In either case the pulsed source would have a far wider overall Q range, which, if needed, might effectively gain a further factor of say two or three in counting time. The same conclusions may be reached by considering the 'band width' arguments presented by Pynn (1995) and Mezei (1994*a*).

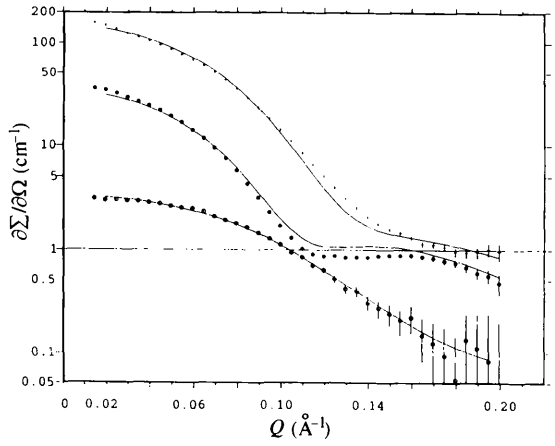

Fig. 11. SANS data from LOQ illustrating model fitting over a broad Q range, simultaneously to three different contrasts: water/DDAB/cyclohexane microemulsions in drop (H/H/D), shell (D/H/D) and core (D/H/H) contrasts. The model has a Schultz polydisperse core, a fixed thickness of surfactant shell, with solvent penetration changing the scattering-length density, and uses simple steps for contrast profile (Eastoe *et al.*, 1996). Absolute intensities are in good agreement with known sample concentrations.

The comparison presented here assumes identical neutron instruments and spectral shapes and ignores practical details of instrument design, such as the relative efficiency of velocity selectors or neutron guides. The shape of the scattering curve to be measured also has some bearing on the argument. For example, a steeply falling 'fractal' structure factor may be easily accommodated on a pulsed source without the need to attenuate the beam to avoid very strong small Q scatter swamping the detector, as the strongest signal comes from the relatively few long-wavelength neutrons. The technical problem of recording ever higher count rates is equally a problem for both pulsed and reactor sources.

Recent progress in the fabrication of grazing-incidence toroidal focusing mirrors, notably for the IN15 spin-echo spectrometer at ILL (Alefeld *et al.*, 1997), promises to provide a route to much smaller Q values with short SANS instruments (Alefeld *et al.*, 1989). Though this will benefit reactors also, such devices will be of particular importance to pulsed sources where frame overlap is to be avoided.

Many modern SANS experiments do demand the wide Q range and good resolution that a pulsed source is able to offer. Fig. 11 illustrates a simultaneous model fit to 'core', 'shell' and 'droplet' contrast data from a water-in-oil microemulsion (Eastoe *et al.* 1996), using data from LOQ. The discrepancies at high Q are due to the limitations of the present model, rather than any systematic effects in the data.

Oriented samples, such as those in shear flow (Cummins *et al.*, 1990), require simultaneous access to a wide Q range to be able to record and fit the anisotropic scattering, without having to repeat difficult experiments at more than one detector position.

7. Conclusions

SANS instruments with accelerator-based pulsed neutron sources have rather different but generally complementary characteristics to those of the more common fixed-wavelength reactor-source instruments. The pulsed source offers a very wide simultaneous Q range, though the count rate at the extremes of the range is always limited. The pulsed source has intrinsically good wavelength resolution, whereas the reactor source has traditionally used a barely acceptable resolution in order to increase flux. Present pulsed-source SANS instruments have fluxes that are already good compared to those of most research reactors, and for particular types of measurement, may be preferable to even the best reactors. The data-reduction scheme and Q resolution curves require careful consideration, but may be routinely implemented in ways that are transparent to users of the facility.

Without any further major technical developments a 'state of the art' 10 Hz, 1 MW, spallation source could be conceived which, with a coupled hydrogen moderator, could produce a total flux approaching that of the ILL second cold source. Such a source has been proposed as one of two targets for a 'European Spallation Source', and also as a second target station for an upgraded ISIS facility. For sophisticated experiments requiring good resolution over a wide simultaneous Q range, an order of magnitude increase in count rates could be acheived. Indeed, there remains scope for considerable improvement of the pulsed source given further development of the technology involved.

References

Alefeld, B., Schwahn, D. & Springer, T. (1989). *Nucl. Instrum. Methods A*, **274**, 210–216.

Alefeld, B., Hayes, C., Mezei, F. Richter, D. & Springer, T. (1997). *Physica B*, **234**, 1052–1054.

Barker, J. G. & Pedersen, J. S. (1995). *J. Appl. Cryst.* **28**, 105.

Broome, T. A., Hogston, J. R., Holding, M. & Howells, W. S. (1994). *Proceedings of ICANS XII.* Report 94–025, pp. T/156–T/163. RAL, Didcot, England.

Carlile, C. J. & Penfold, J. (1995). *Neutron News*, **6**(2), 5–13.

Cotton, J. P. & Teixeira, J. (1986). *Physica B*, **135**, 103–105.

Cummins, P. G., Staples, E., Millen, B. & Penfold, J. (1990). *Meas. Sci. Technol.* **1**, 179–183.

Eastoe, J., Dong, J., Hetherington, K. J., Steytler, D. C. & Heenan, R. K. (1996). *J. Chem. Soc. Faraday Trans.* **92**, 65.

Ghosh, R. E. & Rennie, A. R. (1990). *Inst. Phys. Conf. Ser.* **107**, 233.

Heenan, R. K. (1996). *Q Resolution on LOQ at ISIS*, unpublished report.

Heenan, R. K. & Rennie, A. R. (1994). *Proceedings of ICANS XII.* Report 94–025, pp. I/241–I/247. RAL, Didcot, England.

Ishikawa, Y., Furusaka, M., Niimura, N., Arai, M. & Hasegawa, K. (1986). *J. Appl. Cryst.* **19**, 229–242.

Kiyanagi, Y., Watanabe, N., Furusaka, M., Iwasa, H. & Fujikawa, I. (1990). *Proceedings of ICANS XI.* Report 90–25, pp. 388–400. KEK, Japan.

Kiyanagi, Y., Watanabe, N. & Iwasa, H. (1992). *Nucl. Instrum. Methods A*, **312**, 561–570.

Mezei, F. (1994*a*). *Neutron News*, **5**(3), Editorial, 2–3; see also letter from G. S. Bauer and reply by F. Mezei in *Neutron News*, (1995), **6**(1).

Mezei, F. (1994*b*). *Proceedings of ICANS XII.* Report 94–025, pp. I/377–I/384. RAL, Didcot, England.

Mildner, D. F. R. & Carpenter, J. M. (1984). *J. Appl. Cryst.* **17**, 249–256.

Mildner, D. F. R., Carpenter, J. M. & Worcester, D. L. (1986). *J. Appl. Cryst.* **19**, 311–319.

Ostanevich, Y. M. (1987). *Makr. Chem. Macr. Symp.* **15**, 91–103.

Pedersen, J. S., Posselt, D. & Mortensen, K. (1990). *J. Appl. Cryst.* **23**, 321–333.

Perring, T. G., Taylor, A. D. & Perry, D. R. (1985). Report 85–029. RAL, Didcot, England .

Pynn, R. (1995). In *Proc. Workshop on Neutron Instrumentation for Long Pulsed Neutron Sources*. Report LBL-37880, UC-406, CONF-9504205. Lawrence Berkeley Laboratory, USA.

Rennie, A. R. & Heenan, R. K. (1992). *Proceedings of ISSI Meeting*, pp. 176–184. JINR Dubna, Russia.

Seeger, P. A. (1995). In *Proc. of Workshop on Neutron Instrumentation for Long Pulsed Neutron Sources*. Report LBL-37880, UC-406, CONF-9504205. Lawrence Berkeley Laboratory, USA.

Seeger, P. A. & Hjelm, R. P. Jr (1991). *J. Appl. Cryst.* **24**, 467–478.

Taylor, A. D. (1992). Editor. *Instrumentation and Techniques for the European Spallation Source*. Report 92–040. RAL, Didcot, England.

Teixeira, J. (1992). *Structure and Dynamics of Strongly Interacting Colloids and Supramolecular Aggregates in Solution*, NATO ASI Proceedings, edited by S.-H. Chen, J. S. Huang & P. Tartaglia, pp. 635–658. Dordrecht: Kluwer Academic Publishers.

Wignall, G. D. & Bates, F. S. (1987). *J. Appl. Cryst.* **20**, 28–40.

Windsor, C. G. (1988). *J. Appl. Cryst.* **21**, 582–588; see also other authors in *J. Appl. Cryst.* (1988), **21**, 589–897 and *J. Appl. Cryst.* (1991), **24**, 413–877.